

Article

A Visual-Based Approach for Driver's Environment Perception and Quantification in Different Weather Conditions

Longxi Luo, Minghao Liu, Jiahao Mei, Yu Chen and Luzheng Bi *

School of Mechanical Engineering, Beijing Institute of Technology, Beijing 100080, China; longxiluo@bit.edu.cn (L.L.); 3220220449@bit.edu.cn (M.L.); 3120210414@bit.edu.cn (J.M.); 3220220439@bit.edu.cn (Y.C.)

* Correspondence: bhxblz@bit.edu.cn; Tel.: +86-1368-3184-632

Abstract: The decision-making behavior of drivers during the driving process is influenced by various factors, including road conditions, traffic situations, weather conditions, and so on. However, our understanding and quantification of the driving environment are still very limited, which not only increases the risk of driving but also hinders the deployment of autonomous vehicles. To address this issue, this study attempts to transform drivers' visual perception into machine vision perception. Specifically, the study provides a detailed decomposition of the elements constituting weather and proposes three environmental quantification indicators: visibility brightness, visibility clarity, and visibility obstruction rate. These indicators help us to describe and quantify the driving environment more accurately. Based on these indicators, a visual-based environmental quantification method is further proposed to better understand and interpret the driving environment. Additionally, based on drivers' visual perception, this study extensively analyzes the impact of environmental factors on driver behavior. A cognitive assessment model is established to evaluate drivers' cognitive abilities in different environments. The effectiveness and accuracy of the model are validated through driver simulation experiments, thereby establishing a communication bridge between the driving environment and driver behavior. This research achievement enables us to better understand the decision-making behavior of drivers in specific environments and provides some references for the development of intelligent driving technology.

Keywords: visual perception; environmental quantification; driving simulation; driving behavior modeling



Citation: Luo, L.; Liu, M.; Mei, J.; Chen, Y.; Bi, L. A Visual-Based Approach for Driver's Environment Perception and Quantification in Different Weather Conditions. *Appl. Sci.* **2023**, *13*, 12176. <https://doi.org/10.3390/app132212176>

Academic Editor: Manuel Graña

Received: 8 October 2023

Revised: 4 November 2023

Accepted: 7 November 2023

Published: 9 November 2023



Copyright: © 2023 by the authors. Licensee MDPI, Basel, Switzerland. This article is an open access article distributed under the terms and conditions of the Creative Commons Attribution (CC BY) license (<https://creativecommons.org/licenses/by/4.0/>).

1. Introduction

In recent years, with the continuous development of emerging scientific and technological advancements, such as big data and mobile connectivity, the utilization of onboard sensors has been widely applied. However, under adverse weather conditions, the recognition accuracy of most onboard sensors significantly decreases, posing higher demands on drivers for safety, efficiency, and comfort during the driving experience. For instance, in rainy or snowy weather, the capability of lidar sensors in obstacle detection is noticeably limited, thereby severely impacting driving safety. To ensure the safety and stability of driving in various environments, research on drivers' perceptions and understanding of the environment has become critically important [1].

Nevertheless, environmental research faces two major challenges. Firstly, the complexity of weather conditions makes their quantification a formidable task. Weather phenomena involve multiple variables and interactions, making it difficult to accurately describe weather phenomena. Secondly, the variability of weather makes conducting real-world testing highly challenging. The constantly changing weather conditions increase the uncertainty of the actual testing environment, thereby limiting research on driving environments.

Currently, there is relatively limited work on driving environments, especially concerning weather research. This is mainly due to the difficulty of accurately describing the environment and the challenges associated with conducting practical tests.

The decision-making processes and behavioral patterns exhibited by drivers during the act of driving are subject to the influence of numerous factors, predominantly encompassing the external surroundings and the driver's intrinsic attributes. Consequently, these factors give rise to the emergence of potential hazards and risks within the driving context. The external environment involves moving objects (motor vehicles, nonmotor vehicles, and pedestrians) [2,3], static environmental elements (road boundaries, lane separation lines) [4,5], dynamic traffic control signals (traffic lights) [6], and weather [7–9]. Wang et al. constructed a unified driving safety field model that utilizes field theory to represent risks caused by drivers, vehicles, road conditions, and other traffic factors [10,11]. Tan et al. conducted a unified model of driving behavior in different scenarios. The use of field theory to link the risk steady-state theory and the predictive following theory, two behavioral theories [12], did not consider the impact of environmental factors on driving behavior.

There are many studies on the driver's own factors in relevant studies. The driver's own factors include the driver's driving experience [13,14], the driver's driving style [15–17], the driver's physiological and psychological state, etc. Yang et al. considered the personalized factors of human drivers and the traffic environment and derived a personalized humanoid lane change trajectory planning model [18]. There have been relevant articles proving that the same driver may exhibit different behaviors under different emotions because, under the influence of emotions, the activation direction, intensity, and depth of the nervous system have changed [19]. Under different weather conditions, the driving behavior of the same driver can also change. Zhao et al. analyzed the driving behavior changes and influencing factors of drivers under three different visibility conditions: no fog, light fog, and heavy fog [20]. Jabeer introduced a method of using visual data to detect weather conditions and proposed a weather detection system based on deep learning technology, but did not consider the relationship between driver behavior and the environment [21]. Indeed, weather conditions exert an influence on drivers' perceptual and cognitive faculties, encompassing visual, tactile, and other sensory modalities. The driver's visual perception serves as a crucial conduit for acquiring environmental information, and variations in environmental conditions can significantly influence the driver's sensory experiences. Consequently, these disparities in sensory input can potentially alter the driver's behavioral responses. A schematic representation of the impact of the driving environment on driver behavior is depicted in Figure 1. To establish the logical coherence of this article, the subsequent assumptions are posited.

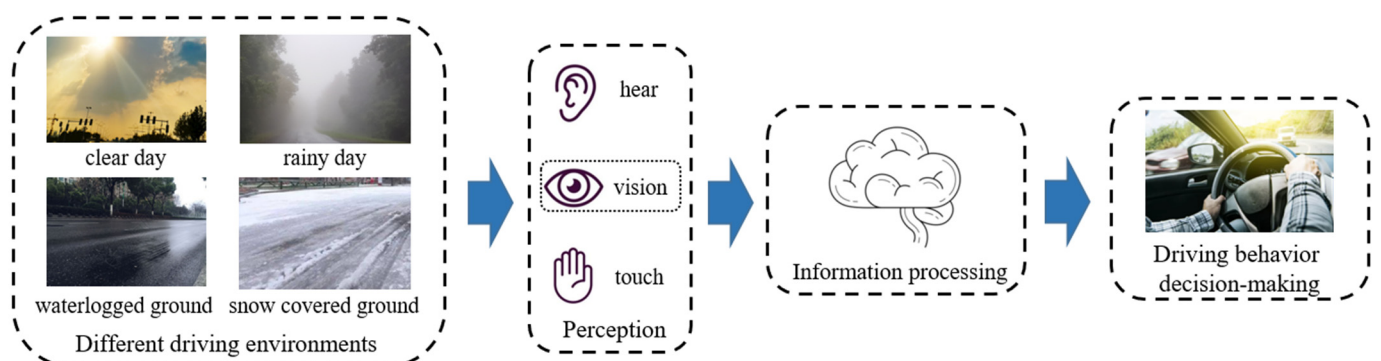


Figure 1. The influence of the environment on behavior.

The remaining sections of this article are presented as follows: In Section 2, we delve into the design of experimental scenarios, experimental paradigms, and the collection of experimental data. Section 3 provides an in-depth exploration of the methodology utilized in this article. This includes a detailed analysis of environmental components, image

feature extraction, quantification methods for environmental indicators, and the selection of driver behavior features. Section 4 introduces the modeling process and evaluation. Section 5 is dedicated to a comprehensive discussion of the driving process under various weather conditions. Section 6 addresses the limitations of our study and summarizes the conclusions drawn from our research. Additionally, we will touch upon potential avenues for future research.

2. Experiment Design

2.1. Experimental Scenario Design

This paper uses the open-source autonomous driving simulator CARLA as a research tool. CARLA provides an experimental environment that enables researchers to build virtual scenarios and test autonomous driving algorithms. The simulator has a variety of sensors and experimental components, including lidar, cameras, GPS, etc. These sensors can simulate real-world perception capabilities and provide an important data source for algorithm development and evaluation.

In this experiment, this paper uses the CARLA simulator and RoadRunner (2022b) for joint simulation to build a virtual scene. Through the integration with RoadRunner (2022b), we can more accurately simulate the real traffic environment and provide more challenging test scenarios. This cosimulation approach can help us study the performance and safety of autonomous driving systems in complex traffic situations. This paper uses the open-source feature of CARLA to independently design elements, such as pedestrians, vehicles, trees, and signs, in the experimental scene. At the same time, we also adjusted the weather element parameters, including rain, snow, fog, etc., to create simulated experimental scenarios under different environmental conditions. Such a setup can help us study the ability of the automatic driving system to cope with various weather and road conditions.

The construction process of the simulated driving platform in this paper includes the installation and configuration of CARLA, the design and placement of scene elements, sensor settings, and the adjustment of experimental scene parameters. Through this process, we are able to establish a highly controlled experimental environment for systematic testing and performance evaluation. The construction process of the simulation driving platform is shown in Figure 2.

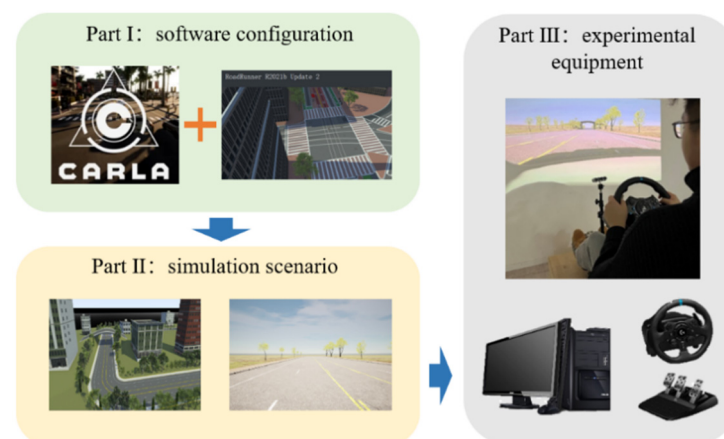


Figure 2. Simulation driving platform and equipment.

To ensure the integrity of the driving process and data, the entire driving process needs to encompass stages of acceleration, deceleration, constant speed, turning, and straight driving [15]. In order to present a more intuitive representation of the simulated driving environment, this paper designs an overhead view of the simulated driving scenario, as shown in Figure 3. In practical simulated driving processes, the scenario primarily includes elements such as roads, bridges, and roadside structures. The design of the scenario takes into consideration the different stages of the driving process and provides corresponding

guidance and prompts. The entire driving scenario can be divided into six stages, each characterized by unique features and driving operation requirements. Detailed descriptions of the six driving stages are listed in Table 1. To guide drivers in their acceleration and deceleration maneuvers, this study incorporates auxiliary facilities such as deceleration signs and brake reminders. For instance, during S3, drivers will receive prompts stating “Please decelerate when approaching the bridge ahead,” and corresponding road signs will be placed on the right side of the road approaching the bridge. These design measures aim to remind drivers to adjust their vehicle speed to safely pass the bridge. Similarly, other stages will also provide relevant guidance and prompts according to specific circumstances, assisting drivers in completing various driving operations.

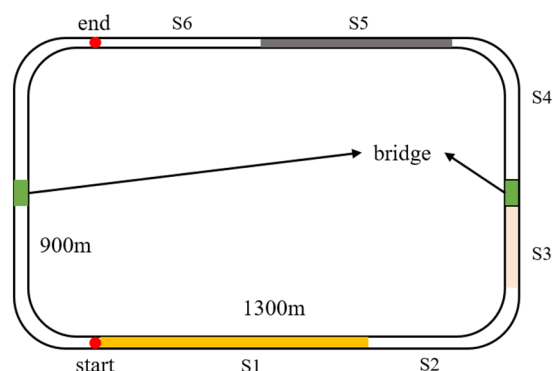


Figure 3. Top view of simulated driving scene.

Table 1. Descriptions of Six Driving Stages.

Stage	Behavior	Description
S1	Accelerate	Accelerate gradually to the limit speed
S2	Decelerate	Bridge ahead, please slow down
S3	Straight	Straight ahead first
S4	Turn	Turning
S5	Uniform Speed	Keep going at your current speed
S6	Parking	Park the vehicle safely

Additionally, the driving scenario design takes into account the inclusion of various road and environmental factors that can affect the driving experience. This includes considering weather conditions, visibility, and road surface conditions, among other factors. By incorporating these elements into the simulated driving scenario, drivers can gain a more realistic and comprehensive understanding of different driving situations. The scenario design also includes the placement of relevant road signs, traffic signals, and landmarks to replicate real-world driving scenarios accurately.

2.2. Experimental Paradigm

This experiment selected experienced drivers with at least one year of driving experience as participants, which means that these drivers have obtained a driving license and completed a one-year driving probation period. This experiment gathered driving data from a cohort of 20 drivers, comprising 15 males and 5 females, whose ages ranged between 20 and 35 years. The average driving experience among the 20 participants surveyed amounted to 5.2 years. This article chose not to establish an age-gradient experimental group for several reasons. First, using a homogenous group of participants of the same age allowed for a more unified and streamlined analysis of the results, thereby increasing the clarity with which conclusions can be drawn from the data. Secondly, the main focus of this paper is to study the impact of weather conditions on driving behavior. Therefore, the decision to maintain consistent age groups was made to mitigate potential confounding factors caused by age-related changes.

Prior to the start of the experiment, drivers received training on the driving simulator to familiarize themselves with its practical operation. After the training was completed, their proficiency was evaluated. For participants who did not pass the pre-experiment training, this article deletes their experimental data and only retains the experimental data of those who passed the training. Subsequently, participants underwent driving simulation experiments in different environments. The experimental site was situated indoors, and throughout the experiment, we diligently strived to minimize potential disruptions or extraneous influences that might impact the driver's concentration while operating the vehicle. During the experiment, drivers were required to perform driving maneuvers based on their personal driving habits and experience. The selection of the experimental timeframe was based on the experimenter's personal considerations, specifically to ensure optimal alertness and energy levels, ranging from 10:00 am to 5:00 pm. Each individual experimental session had a duration of fifteen minutes. Every participant was obliged to undertake two such experiments, with a prescribed ten-minute intermission between them, strategically designed to safeguard the driver's preparedness and physical condition. Throughout the experiment, drivers encountered various driving scenarios and road conditions to simulate real-life driving situations.

The high-definition projection screen of the driving simulator displayed realistic roads and environments, enabling drivers to experience a lifelike driving experience. The operational devices such as the steering wheel, pedals, and gear lever in the driving simulator were similar to those in real vehicles, allowing drivers to perform operations such as steering, acceleration, braking, and gear shifting. The position and angle of the driver's seat could be adjusted according to the driver's personal preference to ensure their comfort and realism within the simulator. A camera located beneath the seat was used to record the driver's facial expressions and driving behavior, which was crucial for subsequent data analysis and evaluation. The driving simulator primarily consisted of the following components: high-definition projection screen, driver's seat, steering wheel, wheelbase, pedals (including clutch, accelerator, and brake), gear lever, connectors, and a computing unit. The driver sat on the driver's seat, positioned 1.2 m away from the central screen, facing forward. A camera was placed beneath the seat to record video data of the driver. The simulated signals generated from the driving maneuvers were converted into electrical signals by the wheelbase and then transmitted to the computing unit. The computing unit was equipped with an i7 processor (Intel® Core™, Santa Clara, CA, USA), 32 GB of memory, and an 8 GB dedicated graphics memory GPU. Table 2 lists the details of the main components of the driving simulator test.

Table 2. Descriptions of Main Components in Driving Simulator Tests.

Device Serial Number	Equipment	Device Description
1	GIMI Z7X (XGIMI Technology, Chengdu, China)	Resolution of 1920 × 1080
2	Logitech G29 (Logitech, Newark, NJ, USA)	Steering wheel, Pedals and Shifter
3	Computing unit (Yokogawa Electric Corporation, Tokyo, Japan)	Intel i7, 32Gb RAM, 8Gb VRAM
4	GPU (Nvidia Corporation, Santa Clara, CA, USA)	NVIDIA GeForce RTX 2060 SUPER
5	Camera (Intel Corporation, Santa Clara, CA, USA)	Intel RealSense D435i
6	Driver seat (Logitech, Newark, NJ, USA)	

2.3. Experimental Data Collection

Calibrating the control components is crucial prior to using a driving simulator, involving several key aspects of optimizing the driving experience from an academic perspective.

Firstly, calibration is required for the brake and accelerator pedals to adjust their minimum and maximum rotation angles as well as sensitivity based on the driver's habits. Such adjustments ensure that the driver achieves a sense of operation in the simulator that aligns with their individual driving habits, thereby enhancing the authenticity and reliability of the simulation experiments. Regarding the steering wheel, parameters such as sensitivity, maximum steering angle, force feedback strength, and damping also need to be adjusted to simulate the handling characteristics of real-world driving.

During the experimental process, driving simulators like CARLA incorporate built-in data collection modules that can collect real-time driving data from the driver. This data includes driving speed, steering wheel angle, throttle, and brake pedal positions, among others, which are then saved for subsequent processing and analysis. The collected data from the simulator primarily encompasses aspects such as mechanical control data, vehicle status, and environmental conditions. Some useful data includes throttle pedal pressure, steering wheel angle, gear lever position, vehicle speed, acceleration, position, engine status, fuel consumption, road conditions, and weather information.

Through these driving simulator experiments, a large volume of driving data can be gathered, covering crucial information, such as the driver's operational behavior, reaction time, and attention allocation. This data is crucial for assessing the driving ability and safety of drivers in different driving scenarios. By analyzing this data, it is possible to gain in-depth insights into the driver's behavior patterns and decision-making processes. Additionally, it enables the study of the driver's ability to respond to emergency situations, adapt to complex traffic environments, and interact with other road users.

3. Methodology

3.1. Analysis of Environmental Composition Elements

Many factors affect driver behavior. By examining the influence of various surrounding environments on the driver's driving behavior in a connected vehicle, it is possible to study how the driver reacts in the absence of changes in traffic signals, lanes, and dynamic or static objects [22]. In this particular study, a series of weather environments were created using the simulation open-source platform CARLA. The weather conditions in CARLA consist of multiple elements that can be manipulated by assigning specific values to each element. Weather elements include sun altitude angle, sun azimuth angle, cloudiness, fog density, fog distance, fog falloff, precipitation, wetness, and precipitation deposits. Thus, different weather environments can be generated. For the purposes of this study, a total of eight weather environments were constructed, each with varying brightness, clarity, and obstacle levels.

The eight weather environments constructed constitute the experimental environment set W , and each environment becomes an element in the set W , as shown in Figure 4.

$$W = \{w_1, w_2, w_3, \dots, w_7, w_8\} \quad (1)$$



Figure 4. Eight weather environment scenes. The eight environments generated by changing the sun's azimuth angle, rain and fog concentration, each with different visual senses.

In different external driving environments, the visual perception of drivers varies according to the characteristics of the environment [23–26]. In order to accurately quantify the features of different environments, we propose three measurement indicators: visual brightness, visual clarity, and visual obstruction. Each indicator is influenced by one or more environmental factors, including natural light intensity, rainfall, and potential obstructions. To study the impact of these indicators on driving behavior, we divided them into high and low levels, namely high visual brightness and low visual brightness, high visual clarity and low visual clarity, as well as high visual obstruction and low visual obstruction. By combining these three indicators, we obtained eight different external weather conditions. Among them, the combination of high visual brightness and high visual clarity represents good weather conditions where drivers can clearly observe the road and surrounding environment. In contrast, the combination of low visual brightness and low visual clarity indicates adverse weather conditions with dim light and blurred vision. Furthermore, in environments with high visual obstruction, various obstructions may limit drivers’ visibility of the road and the surrounding environment. In environments with low visual obstruction, drivers can see the road and surroundings more clearly. Through the research and comparison of these eight different external weather conditions, we can better understand the impact of different environments on drivers’ visual perception.

3.2. Image Feature Extraction

In order to extract features of the driving environment more efficiently, this paper uses a convolutional neural network for feature extraction from image information. The extraction neural network architecture is shown in Figure 5. Unlike conventional convolutional neural networks, this paper incorporates a convolutional block attention module (CBAM) during the training process. The CBAM module calculates attention maps from two different dimensions: channel and space, and then multiplies the obtained attention maps with the input feature maps for adaptive feature refinement [27]. Since CBMA is a lightweight universal module, it can be seamlessly integrated into any CNN architecture without additional overhead and can be trained end-to-end with the basic CNN. The layout of its fused convolutional neural network architecture is shown in Figure 6. Among them, the channel attention module uses average pooling and maximum pooling to aggregate spatial information, which is then processed and input into a multilayer perceptron (MLP), and finally outputs feature F' . Unlike channel attention, the spatial attention module first performs average pooling and maximum pooling operations to aggregate channel information, and finally outputs F'' as a feature map.

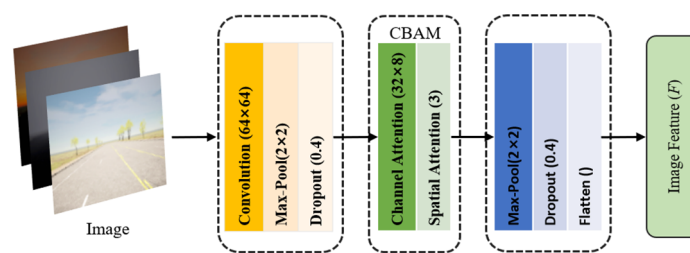


Figure 5. Image feature extraction network.

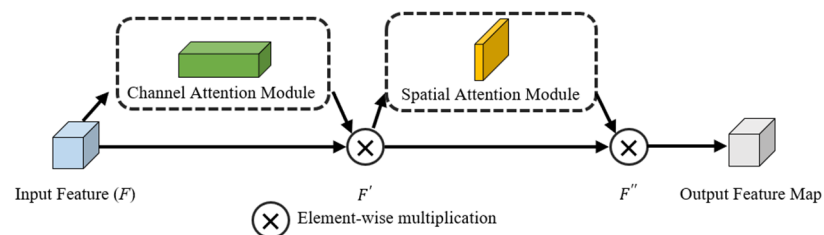


Figure 6. Convolutional block attention module network structure.

The output feature map shows that the pretrained convolutional neural network method can effectively classify different environmental images. The ability to automatically extract features through deep learning enables better understanding and utilization of image data [28]. The generated image features can provide reference, for the selection of environmental quantification indicators in the future.

3.3. Quantitative Methods for Environmental Indicators

This paper utilizes the depth camera and sensors in CARLA to sample eight driving weather conditions, and performs image analysis and quantitative processing on the quantified metrics for each environment. By using CARLA's depth camera and sensors, we are able to capture rich information in various driving weather conditions, including rainy, foggy, and sunny conditions, among others. Through analyzing these sampled data, we can understand the variations in driving scenarios under different weather conditions and extract key quantitative metrics. In the image analysis stage, this study employs computer vision techniques to analyze the sampled images, extracting various visual features and attributes, such as visibility, road conditions, and lighting intensity, to obtain important information about the driving environment. The sampling results are illustrated in Figure 4. Finally, a quantitative processing approach is adopted to convert the information in the images into measurable numerical metrics. By comparing and analyzing these quantitative metrics, we can evaluate different driving weather conditions. Next, this paper will discuss the quantification process of three quantitative indicators.

- (1) Visual brightness. Visual brightness refers to the degree of brightness perceived by the visual sensory system [29], which is influenced by factors such as cloud cover, sun altitude, and azimuth angle. In RGB images, brightness is manifested by the magnitude of pixel values at each point, where higher pixel values indicate higher luminance. In grayscale images, higher grayscale values correspond to higher brightness levels.

In this paper, a method combining RMS pixel height and perceived brightness is used to quantify field-of-view brightness. The pixel height can reflect the reflection (projection) density information of the image, that is, it reflects the brightness information. RMS obtains the root mean square value of the pixel value of each channel in the image, and its calculation formula can be written as:

$$X_{rms} = \sqrt{\frac{1}{N} \sum_{i=1}^n x_i^2} = \sqrt{\frac{x_1^2 + x_2^2 + \dots + x_n^2}{N}} \quad (2)$$

where X_{rms} represents RMS pixel height value. $\{x_1, x_2, x_3, \dots, x_n\}$ represents the pixel height of each channel.

Due to variations in human perception and response to different colors of light when acquiring visual information, researchers have proposed a formula to calculate the "perceived brightness" of individuals based on the relative intensities of three primary colors of light: red, green, and blue. This formula takes into account the differing sensitivities of the human eye to these colors and converts the pixel values of a color image into brightness values that align with human perception [30]. This conversion allows for a more accurate reflection of the human visual system's perception of the image, enabling more precise and rational image processing and analysis. The formula for this calculation can be expressed as:

$$X_{rms-p} = \sqrt{0.241 \times R^2 + 0.691 \times G^2 + 0.068 \times B^2} \quad (3)$$

where X_{rms-p} represents the driver's perceived brightness, R , G , and B represent the three channel colors of red, green, and blue in the image, respectively.

The image brightness is quantified by the above method, and the quantified results are shown in the following Table 3.

Table 3. Visual Brightness Quantification Result.

Weather	X_{rms}	X_{rms-p}
w_1	200.32	199.84
w_2	155.82	156.47
w_3	201.18	201.31
w_4	167.02	167.60
w_5	66.66	59.47
w_6	75.61	76.10
w_7	72.40	63.71
w_8	80.77	81.30

- (2) Visual clarity. Visual clarity is a measure of the level of clarity in a driver’s vision [31], which is influenced by factors such as fog density in the driving environment. When drivers encounter dense fog while driving, higher fog density in the external environment leads to lower visual clarity. In such circumstances, the fog scatters light, preventing drivers from clearly seeing the road conditions, obstacles, and other vehicles ahead. Insufficient visual clarity reduces the driver’s perception of the road and increases the risk of accidents. In this paper, the Laplacian gradient function is used to quantify the driver’s vision clarity.

The Laplacian gradient function employs the Laplacian operator to extract gradient values in both the horizontal and vertical directions. By converging with the image, it obtains the high-frequency components. The high-frequency components are then summed to serve as a measure of image sharpness. The expression for calculating the Laplacian operator and image sharpness is as follows:

$$Laplace(f) = \Delta_f = \frac{\partial^2 f}{\partial x^2} + \frac{\partial^2 f}{\partial y^2} \tag{4}$$

$$D(f)_{lap} = \sum_x \sum_y |G(x, y)|, (G(x, y) > T)$$

where $Laplace(f)$ represents Laplacian operator, $D(f)_{lap}$ represents the image sharpness calculated by the Laplace method, $G(x, y)$ represents pixel point (x, y) of the convolution of the Laplacian operator, T is the given edge detection threshold.

The quantified results are shown in the following Table 4. From the table, it can be seen that the second and fifth weather environments have lower visual clarity, which is consistent with human visual perception.

Table 4. Visual Clarity Quantification Result.

Weather	$D(f)_{lap}$
w_1	131.77
w_2	13.18
w_3	136.17
w_4	182.98
w_5	27.59
w_6	155.95
w_7	180.15
w_8	110.18

- (3) Visual obstruction. During the driving process, external conditions such as rainy or snowy weather may obstruct the driver’s field of vision. Therefore, we propose the concept of visibility obstruction rate as a metric to quantify the extent of visibility obstruction experienced by drivers. The normalized cross correlation (NCC) algorithm, based on grayscale information from images, is a commonly used method for comparing image similarity. The NCC algorithm involves selecting an arbitrary pixel in the original image and constructing a matching window of size $n \times n$. A corresponding

window of the same size is then created at the same location as the target image [32]. By analyzing the similarity between these two windows, the NCC algorithm can ultimately assess the similarity between the two images. This calculation can be expressed as:

$$NCC(p, d) = \frac{\sum_{(x,y) \in W_p} \left(I_1(x, y) - \bar{I}_1(p_x, p_y) \right) * \left(I_2(x + d, y) - \bar{I}_2(p_x + d, p_y) \right)}{\sqrt{\sum_{(x,y) \in W_p} \left(I_1(x, y) - \bar{I}_1(p_x, p_y) \right)^2 * \sum_{(x,y) \in W_p} \left(I_2(x + d, y) - \bar{I}_2(p_x + d, p_y) \right)^2}} \tag{5}$$

Due to the relative nature of occlusion, this paper only compares the impact of rainy weather on visibility occlusion for drivers under the same conditions of clarity and brightness. We separately calculate the occlusion rates of driver visibility in rainy and nonrainy weather. Since the rainfall amount in the simulated rainy environment of this study is constant, the average relative occlusion rate is used to represent the visibility occlusion for drivers in different environments. The quantitative results obtained through the NCC method are presented in Table 5.

Table 5. Visual Obstruction Quantification Result.

Field of View Obstruction	NCC(p,d)
existence	1.566
nonexistence	0.254

3.4. Selection of Driver Behavior Feature Set

For the experimental data of the driver during the driving process, this paper used the difference between the highest speed and the lowest speed, the average speed, the maximum and minimum opening and closing angles of the accelerator, the average opening and closing angle of the accelerator, the brake holding time, and the maximum and minimum angle difference of the brakes. The nine feature sets of the value, the average braking angle, the steering wheel angle interval, and the driving time represent the characteristics of the driver during the driving process. The specific features are expressed in Table 6.

Table 6. Driver Data Feature Set.

Symbol	Feature Description	Unit
v_{max}	maximum speed	m/s
v_{avg}	speed average	m/s
θ_{max}	throttle maximum angle	°
θ_{avg}	throttle average angle	°
δ_{max}	braking maximum angle	°
δ_{avg}	braking average angle	°
η	the proportion of braking time	1
σ	steering wheel angle range	°
t	driving time	s

4. Modeling and Assessment

4.1. Index Normalization and Correlation Analysis

In order to model driver behavior in different environments, it is necessary to further normalize the quantified values obtained through different methods. By using the method of min-max normalization, we can ensure comparability of the quantified values obtained in different environments, thereby facilitating better behavior modeling and analysis. The three environmental data indicators are normalized using the min-max normalization technique, resulting in values within the range [0, 1]. The transformation function is as follows:

$$A^* = \frac{A - min}{max - min} \tag{6}$$

where max represents the data with the largest median value of the environmental index, min represents the data with the smallest value in the environmental index, A represents the quantitative values of each environmental indicator, A^* represents the normalized results of each indicator.

To validate the correlation between different environmental indicators and driver behavior, this study conducted a correlation analysis between driver data and environmental indicators. In the correlation analysis, this paper collected a dataset of driver features and compared it with three quantified environmental indicators.

Table 7 presents the Pearson correlation coefficients between selected driver behavioral features and environmental quantified indicators. All of these coefficients exceed 0.925, indicating that the chosen indicators are accurate and that there exists a strong correlation between driver behavior and the environment. This conclusion also confirms the validity of our model based on assumptions. Based on this conclusion, we conducted a driver's environmental perception and behavior model.

Table 7. Correlation Analysis of Partial Behavioral Feature Sets and Environmental Quantitative Indexes.

Feature Sets	Visual Brightness	Visual Clarity
v_{max}	0.98915	0.98915
v_{avg}	0.93976	0.97302
θ_{max}	0.92844	0.93976
θ_{avg}	0.95742	0.92844
δ_{max}	0.96297	0.95742

4.2. Driver Behavior Modeling

This paper extracts sets of environmental quantification indicators and driving behavior features, and attempts to establish a connection between them using drivers' environmental understanding and behavior models. After the normalization process mentioned above, different driving environments can be represented by three quantified environmental indicators. Therefore, for various environments, a unified quantification formula can be expressed as:

$$A = \alpha \times X_{rms-p} + \beta \times D(f)_{lap} + \lambda \times NCC(p, d) \quad (7)$$

where X_{rms-p} represents visual brightness, $D(f)_{lap}$ represents visual clarity, $NCC(p, d)$ represents visual obstruction. α , β , and λ represent corresponding coefficients.

The behavior of drivers is influenced by environmental factors. One crucial factor is the lighting conditions, which play a significant role in shaping driver behavior. When visibility is excellent due to good lighting conditions, drivers generally exhibit more aggressive behavior on the road. This manifests in their tendency to drive at higher average speeds and brake less frequently. The improved visibility allows drivers to perceive and react to their surroundings more efficiently, potentially leading to a greater sense of confidence and willingness to take risks. Conversely, when faced with poor lighting conditions, such as at night or in inclement weather, drivers tend to adopt a more conservative driving style. The reduced visibility in these situations necessitates caution and careful navigation. Consequently, drivers often drive at lower average speeds and brake more frequently to maintain control and ensure safety.

Recognizing the correlation between driving behavior and lighting conditions, we introduce the concept of the driver conservation factor (DCR). DCR serves as a quantifiable measure to assess the level of conservativeness or aggressiveness in driver behavior. The model-building process is shown in Figure 7. It is determined by calculating the average driving speed, with a higher average speed corresponding to a larger DCR value. This factor allows us to establish a driver behavior model that incorporates the influence of environmental conditions, particularly lighting, on driver decision-making and actions. By considering the interplay between environmental factors and driver behavior, our proposed

model aims to enhance our understanding of how drivers adapt and respond to varying conditions on the road.

$$DCR = \varphi * v_{avg} + \mu * \theta_{avg} + \dots + \varepsilon * \delta_{avg} \quad (8)$$

where DCR represents the driver conservation factor, v_{avg} represents speed average, θ_{avg} represents throttle average angle, δ_{avg} represents braking average angle. φ , μ , and ε represent corresponding coefficient.

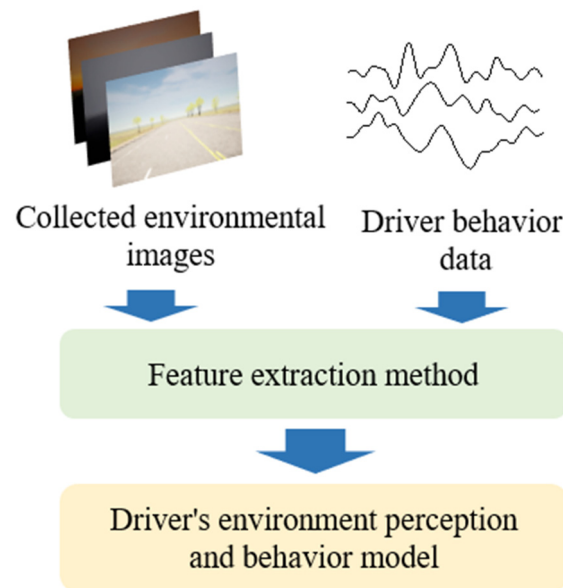


Figure 7. Model Building Process.

The driver behavior characteristics in the driver behavior model can be increased or decreased according to the scene, and at the same time, the coefficients can also be corrected according to the experimental scene and experimental data, which improves the robustness of the model. Verified by experimental data, there is a strong linear correlation between the quantitative value of the environment and the driver's behavior factors, which shows that the model is effective under the premise of the experimental assumption.

5. Discussion

This experiment consisted of six driving stages, and we chose to conduct a detailed analysis of the relationship between the position and velocity of a driver during the acceleration stage, as shown in Figure 8. The figure illustrates the variations in the driver's velocity under different conditions, including visual brightness, visual clarity, and visual obstruction. Based on the observations in the figure, it is evident that the driver's speed is significantly higher under conditions of maximum visual brightness, maximum visual clarity, and minimum visual obstruction compared to other conditions. This indicates a positive impact of favorable visual conditions on the driving speed of the driver. It is worth noting that, during this acceleration process, the frequency of braking by the driver noticeably decreases, highlighting the importance of studying the impact of weather conditions on driving decisions. Additionally, the experiment observed instances where the driver performed braking maneuvers in situations where it was not necessary. Through further analysis, we speculate that this behavior may involve the presence of irrational decision-making by the driver, wherein environmental factors and personal experience could play a significant role. This finding emphasizes the importance of considering the driver's cognition and behavioral patterns, as well as environmental factors, when studying driving behavior and safety.

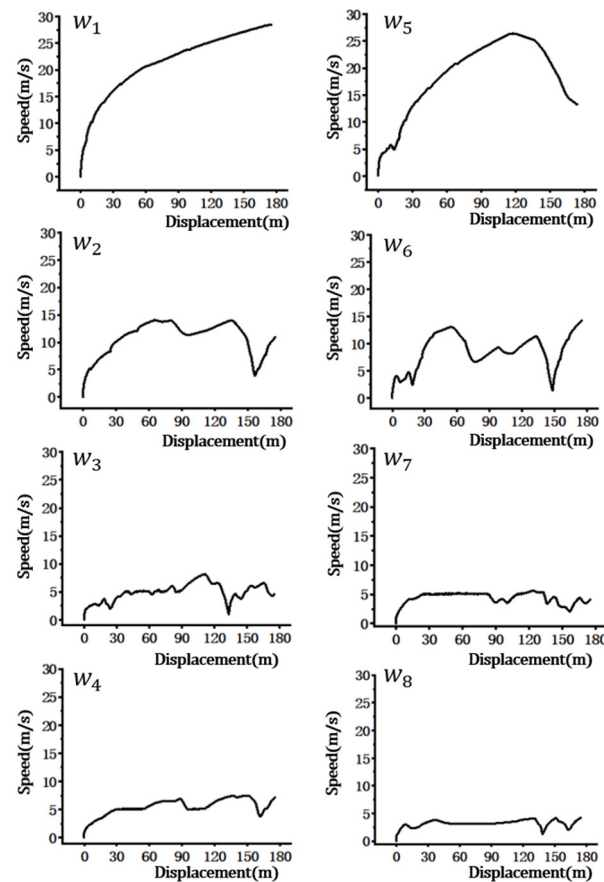


Figure 8. A Diagram of the relationship between speed and displacement of a driver in the acceleration phase.

Studies have demonstrated that inclement weather conditions, such as rain, snow, fog, hail, or strong winds, can significantly diminish road visibility and traction, subsequently influencing driver decision-making and behavior. Drivers may find it necessary to reduce their speed, increase their following distance, or select safer routes. These findings align with the outcomes of our research, which reveal substantial alterations in driver behavior during adverse weather conditions, primarily manifesting as an increased frequency of deceleration and adjustments in speed.

Furthermore, it is worth noting that lighting conditions also exert a substantial influence on a driver's behavior. In accordance with our research findings, enhanced visual brightness corresponds to notable improvements in driving speed and overall driving stability.

6. Conclusions

6.1. Research Summary

This paper mainly has the following contributions and conclusions:

- (1) The paper decomposes the weather components and introduces three environmental quantitative indicators. Additionally, this paper establishes an environmental quantitative method based on the driver's vision. These metrics and methods serve as effective tools for evaluating the driving environment under diverse weather conditions.
- (2) Through simulation experiments conducted in various environments, the paper extracts a comprehensive set of drivers' features and develops a cognitive evaluation model for drivers in different weather conditions. The model provides insights into the behavior patterns exhibited by drivers under distinct weather circumstances.

- (3) Through an examination of weather variables and driver behavior patterns across various weather conditions, it has been determined that drivers exhibit more aggressive driving behavior when visibility conditions are optimal. Furthermore, the extent to which the occlusion rate of the visual field affects the overall environment is considerably less significant than the impact of visual field brightness.

This research contributes to our comprehension of drivers' cognitive processes and their ability to adapt to their surroundings, thereby offering potential avenues for enhancing driving safety.

Due to experimental constraints, the collected driving data in this study cannot represent the driving styles of all drivers. Therefore, the robustness of the mathematical models built based on these data is poor. However, by incorporating additional driver datasets and combining existing machine learning methods, a more accurate mathematical and physical model can be trained. Simultaneously, it is imperative to recognize that this experiment is rooted in simulation, and the dynamics of interaction between individuals and their environment in actual driving scenarios are notably more intricate. Consequently, there exists a need for further investigation into the mechanisms and intensity of such interactions.

Furthermore, while the focus of this experiment is on driver behavior data, future research should pay more attention to drivers' physiological indicators, visual feature indicators, and spatiotemporal feature indicators. For example, wearable devices can be used to collect drivers' physiological data, such as heart rate and conductivity, and analyzing the variations in these indicators can assess the drivers' emotional states and physical conditions. Integrating these multimodal data and indicators can establish a comprehensive model for understanding and predicting driver-environment interactions, thereby better capturing driver behavior patterns and dynamic changes, and enhancing driving safety and experience.

6.2. Research Recommendations and Limitations

The significance of investigating the influence of the driving environment on driving behavior is multifaceted. In light of the research findings presented in this article, several pertinent recommendations emerge:

- (1) Visual brightness, as a key factor among weather-environment indicators, exerts a substantial impact on driving behavior. This observation offers valuable insights for traffic management authorities and researchers, suggesting ways to enhance visual brightness to bolster driving safety in inclement weather conditions.
- (2) Adverse weather conditions can lead to irrational decision-making behaviors among drivers. Consequently, this research bears the potential to guide the formulation of effective traffic regulations and policies that account for the environmental factors influencing driving, including the establishment of specific guidelines tailored to adverse weather conditions.
- (3) This article, to a certain extent, elucidates the model relationship between driving behavior and the driving environment. Within the realm of autonomous driving research, these insights can inform the development of autonomous vehicles and advanced driver assistance systems. These technologies can effectively adapt to diverse driving environments, optimizing transportation systems and mitigating the environmental impact associated with driving.

However, the application of driver simulation experiments to real-world scenarios necessitates a stringent validation procedure to ascertain the viability, safety, and efficacy of the system. For instance, it is imperative to undertake simulation environment verification, which serves to validate the consistency of road and traffic simulations with real-world conditions. Furthermore, the vehicle model utilized in the verification simulation must undergo validation with respect to vehicle dynamics, control systems, and sensors to accurately replicate the vehicle's performance and behavior. Simultaneously, a critical evaluation is essential to confirm the representativeness of the data generated during the simulation process for effective testing and assessment. Moreover, this verification process

extends to encompass security validation, rule verification, and other pertinent aspects. These multifaceted verification measures play a pivotal role in mitigating potential risks and ensuring the adaptability and reliability of autonomous driving technology.

Author Contributions: Conceptualization, M.L. and L.L.; methodology, M.L.; software, L.B.; validation, J.M., Y.C. and L.B.; formal analysis, L.B.; investigation, M.L.; resources, J.M.; data curation, M.L.; writing—original draft preparation, M.L.; writing—review and editing, L.L. and L.B.; visualization, M.L.; supervision, L.L.; project administration, Y.C.; funding acquisition, L.L. All authors have read and agreed to the published version of the manuscript.

Funding: This research was funded by Beijing Natural Science Foundation (grant number 3222021) and Basic Research Plan under grant JCKY2022602C024.

Institutional Review Board Statement: Not applicable.

Informed Consent Statement: Informed consent was obtained from all subjects involved in the study.

Data Availability Statement: Data can be downloaded at this URL: <https://zenodo.org/records/10071069>.

Conflicts of Interest: The authors declare no conflict of interest.

References

- Kolekar, S.; de Winter, J.; Abbink, D. Human-like driving behaviour emerges from a risk-based driver model. *Nat. Commun.* **2020**, *11*, 4850. [[CrossRef](#)] [[PubMed](#)]
- Li, L.; Gan, J.; Ji, X.; Qu, X.; Ran, B. Dynamic driving risk potential field model under the connected and automated vehicles environment and its application in car-following modeling. *IEEE Trans. Intell. Transp. Syst.* **2020**, *23*, 122–141. [[CrossRef](#)]
- Adell, E.; Várhelyi, A.; Dalla Fontana, M. The effects of a driver assistance system for safe speed and safe distance—A real-life field study. *Transp. Res. Part C Emerg. Technol.* **2011**, *19*, 145–155. [[CrossRef](#)]
- Noh, B.; Yeo, H. A novel method of predictive collision risk area estimation for proactive pedestrian accident prevention system in urban surveillance infrastructure. *Transp. Res. Part C Emerg. Technol.* **2022**, *137*, 103570. [[CrossRef](#)]
- Kolekar, S.; Petermeijer, B.; Boer, E.; de Winter, J.; Abbink, D. A risk field-based metric correlates with driver's perceived risk in manual and automated driving: A test-track study. *Transp. Res. Part C Emerg. Technol.* **2021**, *133*, 103428. [[CrossRef](#)]
- Hua, J.; Lu, G.; Liu, H.X. Modeling and simulation of approaching behaviors to signalized intersections based on risk quantification. *Transp. Res. Part C Emerg. Technol.* **2022**, *142*, 103773. [[CrossRef](#)]
- Zhao, L.; Ahmed, A.; Tang, X.; Lin, N.; Liu, C.; Li, J. A weather-assisted driver experiences based path selection method. In Proceedings of the 2018 IEEE 20th International Conference on High Performance Computing and Communications, IEEE 16th International Conference on Smart City, IEEE 4th International Conference on Data Science and Systems (HPCC/SmartCity/DSS), Exeter, UK, 28–30 June 2018; pp. 341–345.
- Malin, F.; Norros, I.; Innamaa, S. Accident risk of road and weather conditions on different road types. *Accid. Anal. Prev.* **2019**, *122*, 181–188. [[CrossRef](#)] [[PubMed](#)]
- Bogaerts, T.; Watelet, S.; Thoen, C.; Coopman, T.; Van den Bergh, J.; Reyniers, M.; Seynaeve, D.; Casteels, W.; Latré, S.; Hellinckx, P. Enhancement of road weather services using vehicle sensor data. In Proceedings of the 2022 IEEE 19th Annual Consumer Communications & Networking Conference (CCNC), Las Vegas, NV, USA, 8–11 January 2022; pp. 1–6.
- Wang, J.; Wu, J.; Li, Y. The driving safety field based on driver-vehicle-road interactions. *IEEE Trans. Intell. Transp. Syst.* **2015**, *16*, 2203–2214. [[CrossRef](#)]
- Wang, J.; Wu, J.; Zheng, X.; Ni, D.; Li, K. Driving safety field theory modeling and its application in pre-collision warning system. *Transp. Res. Part C Emerg. Technol.* **2016**, *72*, 306–324. [[CrossRef](#)]
- Tan, H.; Lu, G.; Liu, M. Risk field model of driving and its application in modeling car-following behavior. *IEEE Trans. Intell. Transp. Syst.* **2021**, *23*, 11605–11620. [[CrossRef](#)]
- Li, T.; Chen, D.; Zhou, H.; Laval, J.; Xie, Y. Car-following behavior characteristics of adaptive cruise control vehicles based on empirical experiments. *Transp. Res. Part B Methodol.* **2021**, *147*, 67–91. [[CrossRef](#)]
- Chen, J.; Sun, D.; Zhao, M.; Li, Y.; Liu, Z. A new lane keeping method based on human-simulated intelligent control. *IEEE Trans. Intell. Transp. Syst.* **2021**, *23*, 7058–7069. [[CrossRef](#)]
- Sharma, A.; Zheng, Z.; Bhaskar, A.; Haque, M.M. Modelling car-following behaviour of connected vehicles with a focus on driver compliance. *Transp. Res. Part B Methodol.* **2019**, *126*, 256–279. [[CrossRef](#)]
- Mohammadnazar, A.; Arvin, R.; Khattak, A.J. Classifying travelers' driving style using basic safety messages generated by connected vehicles: Application of unsupervised machine learning. *Transp. Res. Part C Emerg. Technol.* **2021**, *122*, 102917. [[CrossRef](#)]
- Li, G.; Yang, Y.; Zhang, T.; Qu, X.; Cao, D.; Cheng, B.; Li, K. Risk assessment based collision avoidance decision-making for autonomous vehicles in multi-scenarios. *Transp. Res. Part C Emerg. Technol.* **2021**, *122*, 102820. [[CrossRef](#)]

18. Yang, S.; Zheng, H.; Wang, J.; El Kamel, A. A personalized human-like lane-changing trajectory planning method for automated driving system. *IEEE Trans. Veh. Technol.* **2021**, *70*, 6399–6414. [[CrossRef](#)]
19. Lee, M.; Lee, S.; Hwang, S.; Lim, S.; Yang, J.H. Acquiring Driving Characteristic Data According to Driver Emotions and Proposing Emotion Groups in the Driving Context. In Proceedings of the 2022 IEEE 3rd International Conference on Human-Machine Systems (ICHMS), Orlando, FL, USA, 17–19 November 2022; pp. 1–7.
20. Zhao, X.; Chen, Y.; Li, H.; Ma, J.; Li, J. A study of the compliance level of connected vehicle warning information in a fog warning system based on a driving simulation. *Transp. Res. Part F Traffic Psychol. Behav.* **2021**, *76*, 215–237. [[CrossRef](#)]
21. Jabeen, S.; Malkana, A.; Farooq, A.; Khan, U.G. Weather classification on roads for drivers assistance using deep transferred features. In Proceedings of the 2019 International Conference on Frontiers of Information Technology (FIT), Islamabad, Pakistan, 16–18 December 2019; pp. 221–2215.
22. Ali, F.; Khan, Z.H.; Gulliver, T.A.; Khattak, K.S.; Altamimi, A.B. A Microscopic Traffic Model Considering Driver Reaction and Sensitivity. *Appl. Sci.* **2023**, *13*, 7810. [[CrossRef](#)]
23. Selvaraj, D.C.; Hegde, S.; Amati, N.; Deflorio, F.; Chiasserini, C.F. A Deep Reinforcement Learning Approach for Efficient, Safe and Comfortable Driving. *Appl. Sci.* **2023**, *13*, 5272. [[CrossRef](#)]
24. Christopoulos, S.-R.G.; Kanarachos, S.; Chronos, A. Learning driver braking behavior using smartphones, neural networks and the sliding correlation coefficient: Road anomaly case study. *IEEE Trans. Intell. Transp. Syst.* **2018**, *20*, 65–74. [[CrossRef](#)]
25. Pauwelussen, J.; Feenstra, P.J. Driver behavior analysis during ACC activation and deactivation in a real traffic environment. *IEEE Trans. Intell. Transp. Syst.* **2010**, *11*, 329–338. [[CrossRef](#)]
26. Al-Sultan, S.; Al-Bayatti, A.H.; Zedan, H. Context-aware driver behavior detection system in intelligent transportation systems. *IEEE Trans. Veh. Technol.* **2013**, *62*, 4264–4275. [[CrossRef](#)]
27. Muhtar, Y.; Muhammad, M.; Yadikar, N.; Aysa, A.; Ubul, K. FC-ResNet: A Multilingual Handwritten Signature Verification Model Using an Improved ResNet with CBAM. *Appl. Sci.* **2023**, *13*, 8022. [[CrossRef](#)]
28. Woo, S.; Park, J.; Lee, J.-Y.; Kweon, I.S. Cbam: Convolutional block attention module. In Proceedings of the European Conference on Computer Vision (ECCV), Munich, Germany, 8–14 September 2018; pp. 3–19.
29. Gao, S.; Wang, H.; Xue, C. The Effects of Brightness Difference on Visual Perception of Characters. In Proceedings of the 2021 22nd IEEE International Conference on Industrial Technology (ICIT), Valencia, Spain, 10–12 March 2021; pp. 1200–1204.
30. Ji, X.; Guo, S.; Zhang, H.; Xu, W. Non-Uniform-Illumination Image Enhancement Algorithm Based on Retinex Theory. *Appl. Sci.* **2023**, *13*, 9535. [[CrossRef](#)]
31. Ji, X.; Cheng, J.; Bai, J.; Zhang, T.; Wang, M. Real-time enhancement of the image clarity for traffic video monitoring systems in haze. In Proceedings of the 2014 7th International Congress on Image and Signal Processing, Dalian, China, 14–16 October 2014; pp. 11–15.
32. Khan, O.; Muzzammel, R.; Tahir, U.; Azeem, O.; Arshad, R.; Umer, M. Implementation and Comparative Analysis of Semi-Automated Surveillance Algorithms in Real Time using Fast-NCC. In Proceedings of the 2021 International Conference on Innovative Computing (ICIC), Lahore, Pakistan, 9–10 November 2021; pp. 1–6.

Disclaimer/Publisher’s Note: The statements, opinions and data contained in all publications are solely those of the individual author(s) and contributor(s) and not of MDPI and/or the editor(s). MDPI and/or the editor(s) disclaim responsibility for any injury to people or property resulting from any ideas, methods, instructions or products referred to in the content.